Karlsruhe Institute of Technology

Crack growth exponent n for water-vapour soaked silica

Günter Schell, Theo Fett

KIT SCIENTIFIC WORKING PAPERS 74

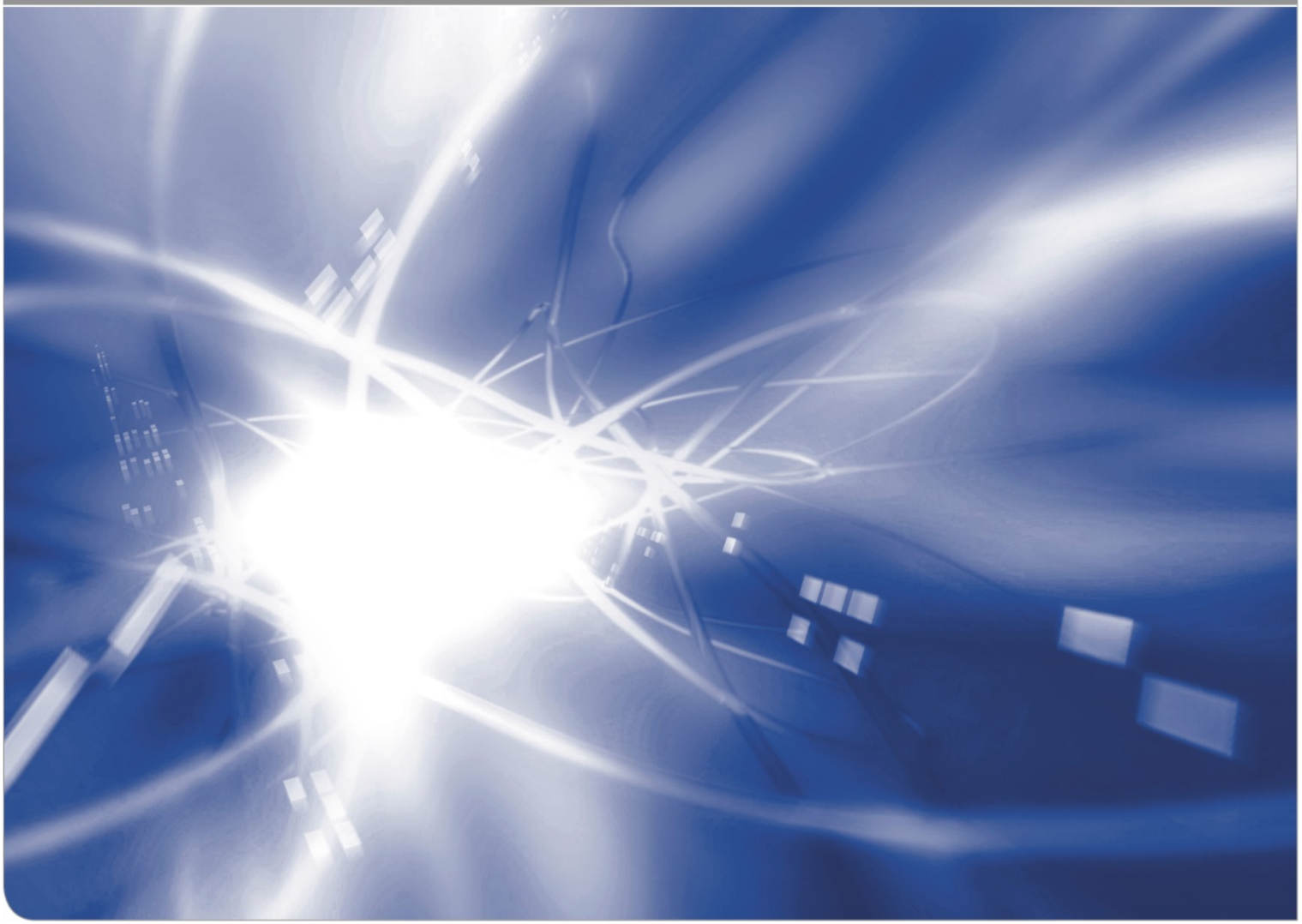

Institute for Applied Materials – Ceramic Materials and Technologies

Impressum

Karlsruher Institut für Technologie (KIT)
www.kit.edu

2017

ISSN: 2194-1629

Abstract

The effect of water soaking on the strength of silica glass is often studied in literature. When silica glass is immersed in warm water or water vapour and held there for an extended period of time, the strength increases over that of freshly damaged glass. The increase in strength is a consequence of water diffusion into exposed surfaces of the test specimen, which results in swelling of the glass and shielding of cracks present in the surface of the glass.

For strength tests carried out in humid environment at various loading rates, so-called dynamic strength tests, we can simply show theoretically that the swelling effect by the reaction of water with silica must result in apparently increased crack-growth exponents. This prediction is in good agreement with results from literature

Contents

1. Introduction

In earlier publications [1-4], the idea was explored that water can toughen silica glass by diffusing into the glass and reacting with the glass structure. This process sets up a compressive stress in the water-affected zone resulting in a negative stress intensity factor that shields the crack tip and enhances the strength of the specimen. Because diffusion rates increase with temperature, crack tip shielding should also intensify as the temperature is increased, as should the specimen strength.

Li and Tomozawa [5] soaked silica bars for up to 4 days and measured the strengths using dynamic bending tests in the presence of water, which enhances subcritical crack growth. Exposure to water at 250 °C enhanced the inert strength and also the strength tested under subcritical crack growth conditions in the presence of water. The main interesting effect found in these tests was an increase of the exponent n of the power law representation with increasing soaking duration. It could be qualitative shown in [1] that the apparently increased n'-value is an artifact of the logarithmic representation of a shift of a straight line by a constant stress. In this note we will show this quantitatively, too.

Water diffusion into the surface of silica glass has been studied experimentally by a number of investigators, and shown to depend on temperature according to

$$D_w = A_0 \exp[-Q_w / RT] \tag{1.1}$$

where Q_w is the activation energy for diffusion, T=(θ+273°) is the absolute temperature in K and θ in °C, and R is the universal gas constant. As reported in reference [6] for silica, $Q_w = 72.3$ kJ/mol, $\log_{10} A_0 = 8.12$ (A_0 is in m^2/s) for the *effective* diffusivity in the temperature range 0 °C to 200 °C.

The diffusion depth b is an appropriate measure for the thickness of the diffusion zone. For the depth b the water concentration is roughly half of that at the surface:

$$b = \sqrt{D_w t} \tag{1.2}$$

The parameter, t, is the time after the first contact with water.

The water in the diffusion zone reacts with the silica network according to the chemical reaction:

$$\equiv\text{Si-O-Si}\equiv + H_2O \leftrightarrow \equiv\text{SiOH} + \text{HOSi}\equiv. \tag{1.3}$$

The moleculer water, H_2O, is fully mobile, and the hydroxyl groups, ≡SiOH, are immobile, fixed at the point of reaction with the silica network. The concentration of the hydroxyl groups is denoted as $S = [\equiv\text{SiOH}]$,

From measurements of curvature of water-soaked silica disks and the related bending moments by Wiederhorn *et al.* [7] it can be concluded that water in silica glass results

in a volume swelling strain ε_v governed by the hydroxyl concentration S exclusively. The swelling strain expressed in weight units of S it holds [8]

$$\varepsilon_v = \kappa \times S \ , \quad \kappa = 0.97 \ [0.92,1.02] \tag{1.4}$$

with the 95%-Confidence Interval in brackets.
A volume element near the surface that undergoes swelling cannot freely expand. If the diffusion zone is small compared to the component dimensions, expansion is completely prevented in the surface plain and can only take place normal to the surface. This results in a compressive equi-biaxial swelling stress at the surface,

$$\sigma_{sw,0} = -\frac{\varepsilon_v E}{3(1-\nu)} \ , \tag{1.5}$$

where E is Young's modulus and ν is Poisson's ratio. For cracks existing in the surface region a shielding stress intensity factor K_{sh} is caused by the swelling stresses. The shielding stress intensity factor can be described as

$$K_{sh} = 1.122\sqrt{\pi a}\,\sigma_{sw,0} F(b/a) \tag{1.6}$$

with a geometric function F depending on the ratio of diffusion zone width b and crack depth a.

2 Dynamic strength affected by swelling stresses

2.1 Edge cracks as defects

The most transparent description of crack-growth problems can be given by using a solution for one-dimensional edge cracks. Under an applied stress σ_{app} the related applied stress intensity factor is

$$K_{appl} = 1.122\sqrt{\pi a}\,\sigma_{appl} \tag{2.1}$$

The geometric function for an edge crack was determined by FE-computations as

$$F(b/a) \cong \tanh^{3/2}\left(\left[0.385\sqrt{\frac{b}{a}} + 0.832\frac{b}{a}\right]^{2/3}\right) \tag{2.2}$$

with the thickness of the swelling zone b given by eq.(1.2). Details for this equation are given in the Appendix.
The crack-tip stress intensity factor K_{tip}, responsible for the singular stresses in the crack-tip region, results by superposition of the applied and shielding stress intensity factors:

$$K_{tip} = K_{appl} + K_{sh}, \ \text{where } K_{sh} < 0 \tag{2.3}$$

Very often subcritical crack growth rates, v, are represented by a power law relation

$$v = \frac{da}{dt} = AK_{tip}^{n} = A(K_{appl} + K_{sh})^{n} \tag{2.4}$$

In the absence of swelling, $\sigma_{sw} = 0$ and $K_{sh} = 0$, the following well-known equation holds [9]:

$$\sigma_{f,0} = \lambda \dot{\sigma}^{1/(n+1)}, \quad \lambda = [B\sigma_c^{n-2}(n+1)]^{1/(n+1)}. \tag{2.5}$$

The subscripts $_0$ in $\sigma_{f,0}$ and $\sigma_{c,0}$ stand for absence of swelling. B is the well-established crack-growth parameter summarizing fracture mechanics parameters, toughness and crack-growth data A and n.

As a consequence of the large n-value for silica (n>30), eq.(2.4) makes clear that the largest stress increments $d\sigma_{appl}$ per crack length increment da occur at the initial crack depth $a \approx a_0$. This follows from $d\sigma_{appl} = \dot{\sigma}\,dt$, and $da = AK^n dt$ via $d\sigma_{appl}/da \propto 1/K^n$. The geometric function can be assumed to be constant: $F(b/a) \cong F(b/a_0)$.

In the presence of swelling, we obtain then the following equations:

$$[\sigma_f + F(\tfrac{b}{a_0})\,\sigma_{sw,0}]^{n+1} = \lambda^{n+1}\dot{\sigma} \tag{2.6}$$

or

$$\Rightarrow \sigma_f = \lambda \dot{\sigma}^{\,1/(n+1)} - F(\tfrac{b}{a_0})\sigma_{sw,0} \tag{2.7}$$

2.2 Semi-circular and semi-elliptical surface cracks as defects

The derivation of strength expressions for other crack shapes is identical as has been outlined for edge cracks. The geometric function $F(b/a_0)$ has of course to be replaced by those for the special type of crack. For the semi-circular crack it holds for the deepest point (A) and the surface points (B) [10]:

$$K_{sh,A,B} \cong \sqrt{a}\,\sigma_{sw,0} F_{A,B}\left(\tfrac{b}{a_0}\right) \tag{2.8}$$

$$F_A(\tfrac{b}{a_0}) = 1.17 \tanh\left(0.698\sqrt{\frac{b}{a_0}} + 0.317\frac{b}{a_0}\right) \tag{2.9}$$

$$F_B(\tfrac{b}{a_0}) = 1.29 \tanh\left(1.327\sqrt{\frac{b}{a_0}} + 0.064\frac{b}{a_0}\right) \tag{2.10}$$

(see also Fig. A3). Since the stress intensity factors at the deepest point and the surface points are different it is impossible that the crack will maintain its shape during extension. The equilibrium shape will become a semi-ellipse with an aspect ratio of $a/c \neq 1$ [10] (c=half crack width). A solution for $K_{A,B}$ was given in [11] and is reported in Appendix A2.

3 Apparent power-law exponent n'

Whereas for the un-soaked material the exponent in the power-law relation, n, can simply be obtained from the slope of the $\sigma_f = f(\dot{\sigma})$ plot, this is no longer possible for the water-vapour soaked material as can be easily shown.

A straight-line evaluation of eq.(2.7) must result in an apparent crack exponent n' defined by

$$\sigma_f = -F(\tfrac{b}{a_0})\sigma_{sw,0} + \lambda\dot{\sigma}^{1/(n+1)} \Rightarrow \sigma_f \propto \dot{\sigma}^{1/(n'+1)} \tag{3.1}$$

or equivalently

$$\frac{1}{n'+1} = \frac{d(\log\sigma_f)}{d(\log\dot{\sigma})} = \frac{d[\log(\lambda\dot{\sigma}^{1/(n+1)} - F(\tfrac{b}{a_0})\sigma_{sw,0})]}{d(\log\dot{\sigma})} \tag{3.2}$$

By using logarithmic derivations, $d(\log x)=(1/x)\,dx$, we obtain the following equation:

$$n' = n + (n+1)\frac{-F(\tfrac{b}{a_0})\sigma_{sw,0}}{\sigma_{f,0}} = n + (n+1)\frac{\sigma_f - \sigma_{f,0}}{\sigma_{f,0}} \quad . \tag{3.3}$$

Since $\sigma_{sw} < 0$, it follows that $n' > n$. Thus, the apparently increased n'-value is an artifact of the logarithmic representation of a shift of a straight line by a constant value $|\sigma_{sw}|$.

4 Comparison with experimental data from literature

As an example of application eq.(3.3), a result from literature may be discussed. Li and Tomozawa [5] investigated the effect of temperature on the dynamic fatigue behavior of silica glass for soaking at 250 °C under saturated vapor pressure. All their strength measurements were performed at room temperature, in air at a relative humidity of 15 % to 30 %. The material tested was a grade of industrial silica, TO8, Heraeus-Amersil Inc. The strength data after different soaking times are in Fig. 1a.

The dynamic strength measurements are plotted in Fig. 1b in form of normalized strength increments as function of exposure time t (squares in Fig. 1b). The curve is tentatively introduced as a guideline to the squares representing a soaking-time dependency of $t^{1/4}$ since for short time $K_{sh} \propto \sqrt{b} \propto t^{1/4}$.

A further interesting result found by Li and Tomozawa [5] was the observation that the crack growth exponent of the v-K_{Ic} curve increased with exposure time. The circles in Fig. 1c show the reported exponents as a function of the strength increase for a stress rate of $d\sigma_{appl}/dt = 10$ MPa/s. The perpendicular bars represent the standard deviations as reported in [5]. The straight line shows the predictions by eq.(3.3). Li and Tomozawa [5] discuss the increase in n as a consequence of "crack-tip blunting".

For comparison, we have to take into account the large data scatter in Fig. 1c, and, consequently, a large uncertainty of the experimental n'-values. For a comparison of

measured and computed n-values in Fig. 1, we determined the confidence intervals of the values $1/(n'+1)$ from Fig. 1a. From the limits of these intervals we computed the related limits for n'. Whereas the intervals for $1/(n'+1)$ are symmetric, those for n are strongly non-symmetric. The 50%- and 90%-confidence intervals (CI) are compiled in Table 1. These intervals are also plotted in Fig. 1c. Li and Tomozawa [5] reported for soaking times of 0 and 4 days the same interval as we found for 50% confidence levels. Confidence levels of 50% are not very often used for data assessment. For this purpose mostly 90% or 95% levels are applied.

Time	σ_f (MPa)	σ_f-$\sigma_{f,0}$ (MPa)	n'	50% CI	90% CI
0 d	59.7	0	32.7	[29.7, 37.9]	[21.8, 63.7]
1 d	149.3	89.6	40.4	[33.4, 50.9]	[23.06, 147]
3 d	183.4	123.7	80.4	[64.2, 107]	[42.1, >1000]
4 d	207.0	147.3	91	[75.1, 116]	[51.4, 380]

Table 1 Evaluation of the strength data from Fig. 1a with confidence intervals for crack-growth exponents n'.

On the basis of the 90%-CI, we conclude from Fig. 1c that the theoretical prediction and the experimental results by Li and Tomozawa [5] are in agreement, i.e. the crack growth exponent increases as expected from eq.(3.3). Since the geometric function is $F(b/a)\leq 1$, the swelling stress at the surface must be $|\sigma_{sw}|\geq 147.3$ MPa.
Figure 2 shows the predictions by introducing into Fig. 1c. This representation states that the predicted straight-lines according to eq.(3.3) are in good agreement with the measurements. This can be seen especially for the strengths after 1 day soaking because in this case the standard deviations were given in [5].

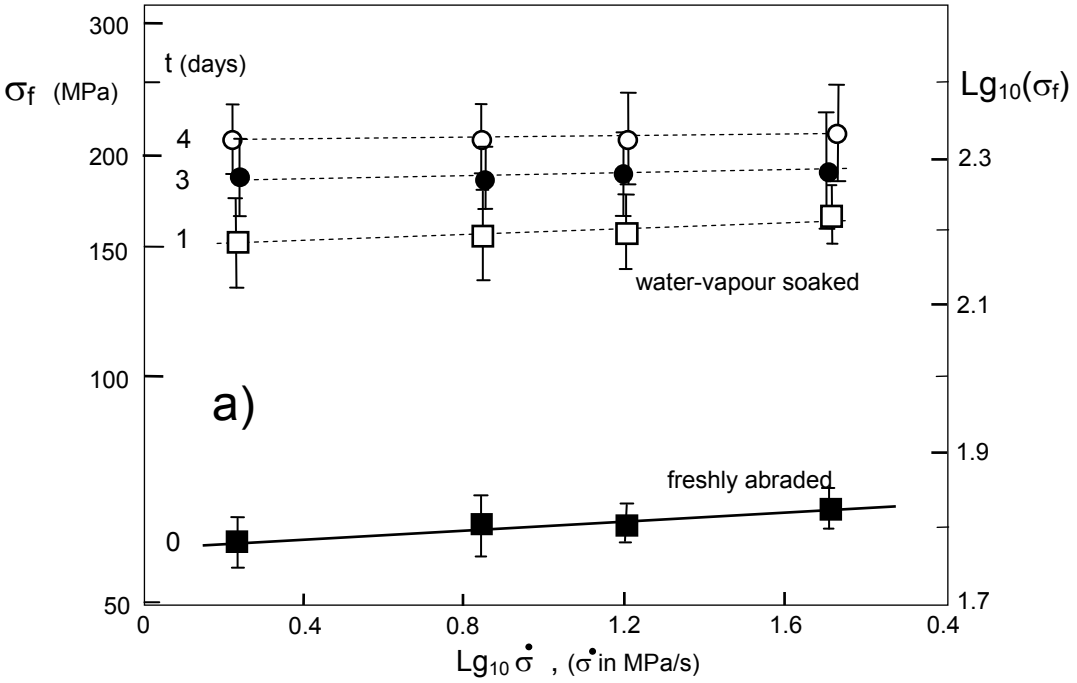

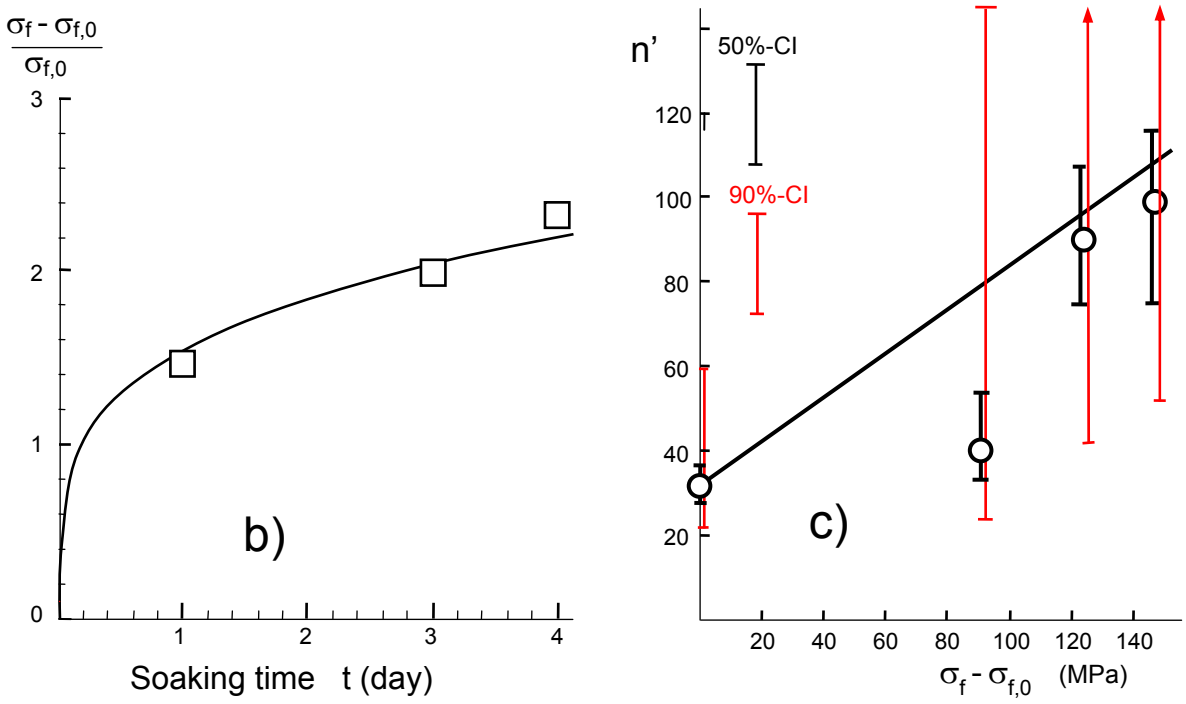

Fig. 1 a) Dynamic bending strength tests by Li and Tomozawa [5] (for clarity the symbols and scatter bars show slightly displaced abscissa values), b) normalized increase of dynamic strength versus heat-treatment time at 250°C; Squares: results from [5], curve: tentatively introduced guide line to the squares representing a dependency $\propto\sqrt{b} \propto t^{1/4}$, c) *n*'-values reported in [5] (circles), straight line: eq.(3.3).

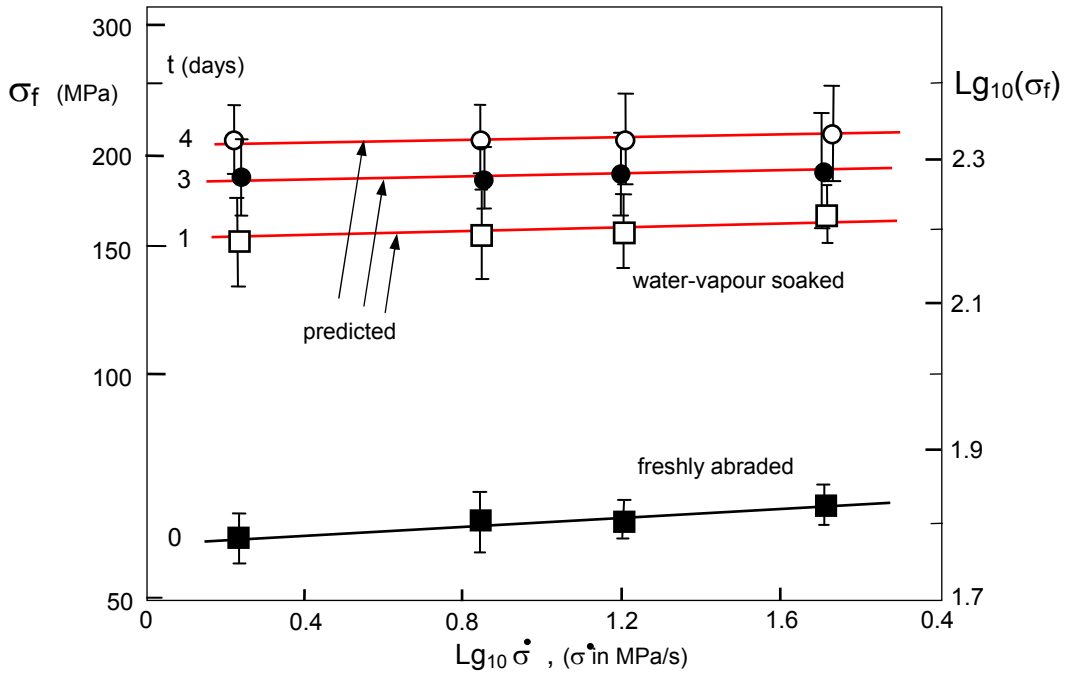

Fig. 2 Predicted straight lines (red) according to eq.(3.3) introduced by the red lines.

An equivalent representation of the agreement between experiment and prediction is given in Fig. 3 where the measured strengths are plotted again with a linear ordinate scaling. The black curve represents the power-law equation (2.4) with n=32.7. In a

linear plot this curve is of course no longer a straight line. The small curvature is hardly visible.

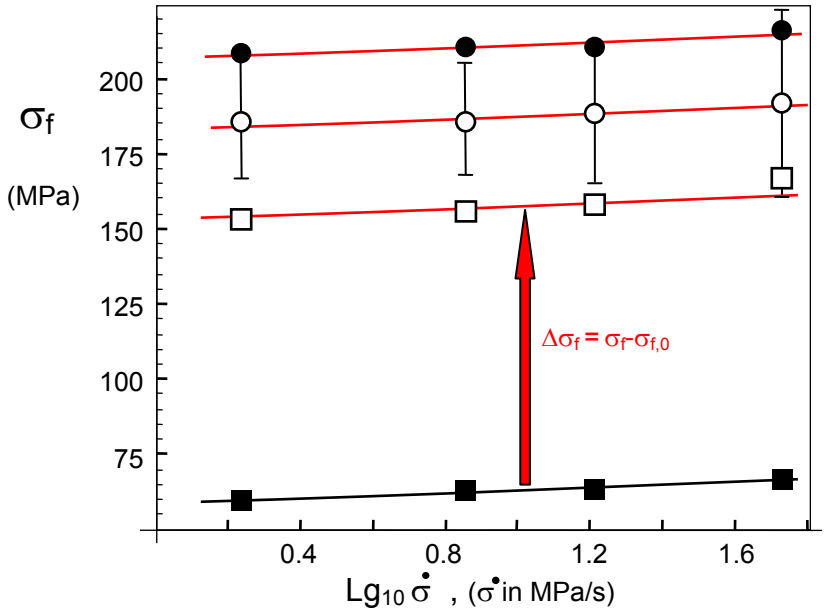

Fig. 3 Data of Fig. 2 represented with linear ordinate scaling (note that curves are no longer straight). Red curves agree with the black one shifted by a constant stress $\Delta\sigma_f$.

The red curves are identical with the black one but shifted by constant stress values $\Delta\sigma_f$ (indicated by the arrow in Fig. 3). From this plot it can be concluded that the shifted curves agree with the measurements that within the natural data scatter (standard deviation bars given for 3 days soaking exclusively). This confirms again the dependency eq.(3.1), namely

$$\sigma_f = \underbrace{-F(\tfrac{b}{a_0})\sigma_{sw,0}}_{\Delta\sigma_f} + \underbrace{\lambda\dot{\sigma}^{\,1/(n+1)}}_{\sigma_{f,0}}$$

or

$$\Rightarrow \sigma_f - \Delta\sigma_f = \lambda\dot{\sigma}^{\,1/(n+1)}$$

Summary:

The present note dealt with the influence of swelling stresses and shielding stress intensity factors for natural cracks in silica, both caused by the reaction between SiO_2 and water.

We considered the effect of swelling stresses on the crack-growth exponent of the power-law for subcritical crack growth. It could be shown that the apparent exponent *n'* of a power law description according to

$$v \propto K_{appl}^{n'}$$

must decrease with increasing swelling. This theoretical consequence of swelling in silica is in rather good agreement with experiments from literature.

For the swelling stress at the surface we obtained for the 4-days soaking tests in [5] a swelling stress of: $|\sigma_{sw}| \geq 147.3$ MPa.
The analysis was explained for the case of edge cracks. The same type of description via eq.(3.3) also holds for half-penny shaped surface cracks with geometric functions given in [4].

APPENDIX:

A1 Shielding stress intensity factor for the edge-cracked half-space

Finite Element computations were carried out for a small edge crack in a rectangular bending bar, a/W=0.005, under plane strain conditions, Fig. A1a. The plate height was chosen as H/W=2 representing sufficiently the infinitely long bar. Swelling was assumed taking place from both specimen side-surfaces. Figure A1b represents the shielding stress intensity factor as a function of b/a. The FE results are introduced as the circles.

In order to obtain an appropriate fitting relation the analytically known limit values have to be included.

For $b/a \to 0$ it was derived in [3]:

$$K_{sh} = -\psi \frac{\varepsilon_v E}{1-\nu}\sqrt{b} - \frac{\varepsilon_v E}{3(1-\nu)}\frac{1.465\,b}{\sqrt{a}} \qquad \text{(A1)}$$

with $\psi \cong 0.255$. The first term reflects the swelling zone along the crack surface. Its value was given by McMeeking and Evans [12] and was determined in [3] also by FE-computations.

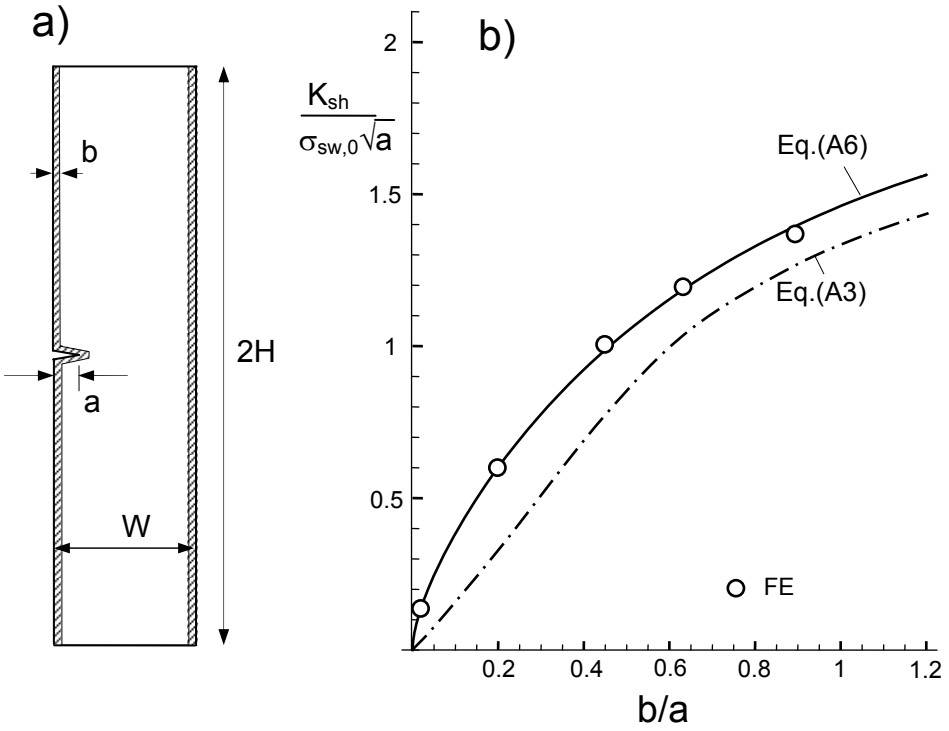

Fig. A1 Finite Element results (circles) compared with the interpolation relation of Eq.(A6), dash-dotted curve: contribution of the side-surface swelling zone.

The derivation of the second term in (A1) may be briefly addressed.

Under the assumption of an erfc-shaped swelling strain distribution extending from the specimen surface, the swelling stresses are

$$\sigma_n \cong \sigma_{sw,0}\,\mathrm{erfc}\left[\frac{x}{2b}\right] \tag{A2}$$

with the compressive surface stress $\sigma_{sw,0}<0$ according to eq(1.5). The contribution of this layer to the shielding stress intensity factor can be computed as

$$K_{sh,surface} = \int_0^\infty \sigma_n h(x,a)dx \tag{A3}$$

with the normal stress σ_n on the crack and the weight function h as given e.g. in [13]. Figure A2 shows h for a crack in the half-space. For very thin swelling zones, $b/a<<1$, it holds $h=1.465/\sqrt{a}$.

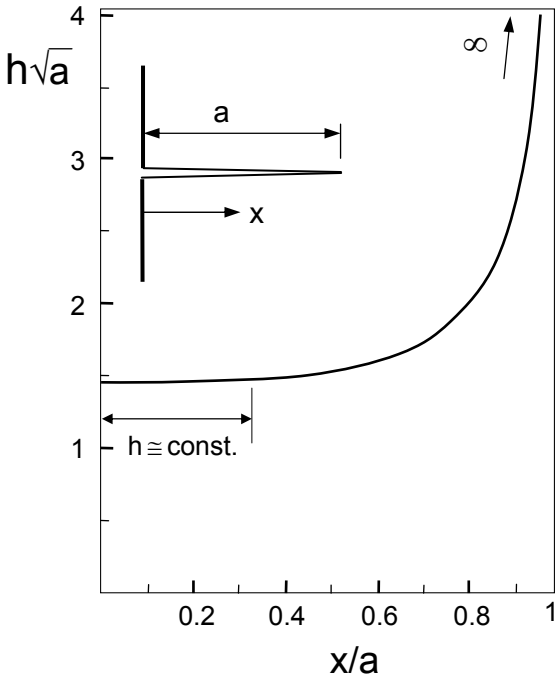

Fig. A2 Weight function h for an edge-cracked half-space.

The shielding stress intensity factor $K_{sh,surface}$ for $b<<a$ then reads

$$K_{sh,surface} \overset{b/a\to 0}{\sim} \sigma_{sw,0}\frac{2}{\sqrt{\pi}}\frac{1.465b}{\sqrt{a}} \tag{A4}$$

which is about 12% larger than the solution for a step-shaped swelling distribution. For the limit $b/a>>1$ it holds

$$K_{sh} = \sigma_{sw,0}F\sqrt{\pi a} \tag{A5}$$

with $F=1.1215$. The solid curve in Fig. A1b represents an interpolation relation including the limit cases that fits best to the FE-results within $0\le b/a\le 1$:

$$K_{sh} \cong 1.122\sqrt{\pi a}\,\sigma_{sw,0}\tanh^{3/2}\left([0.385\sqrt{\frac{b}{a}}+0.832\frac{b}{a}]^{2/3}\right) \tag{A6}$$

The infinity sign stands for the fact that the modeled bar represents practically a semi-infinite body. The dash-dotted curve represents the contribution caused by the side-surface swelling zone exclusively. For $b/a>1$ this contribution counts for more than 90% of the total shielding stress intensity factor.

A2 Semi-circular crack in the half-space via FE

The geometry and shielding stress intensity factors from FE-computations on a semi-circular crack in the semi-infinite body are shown in Fig. A3. The asymptotic limits are well known (upper limit for point B: 1.29, for point A: 1.17). The bold interpolation curves are given as [10]

$$K_{sh,B} \cong 1.29\sqrt{a}\,\sigma_{sw,0}\tanh\left(1.327\sqrt{\frac{b}{a}}+0.064\frac{b}{a}\right) \tag{A7}$$

$$K_{sh,A} \cong 1.17\sqrt{a}\,\sigma_{sw,0}\tanh\left(0.698\sqrt{\frac{b}{a}}+0.317\frac{b}{a}\right) \tag{A8}$$

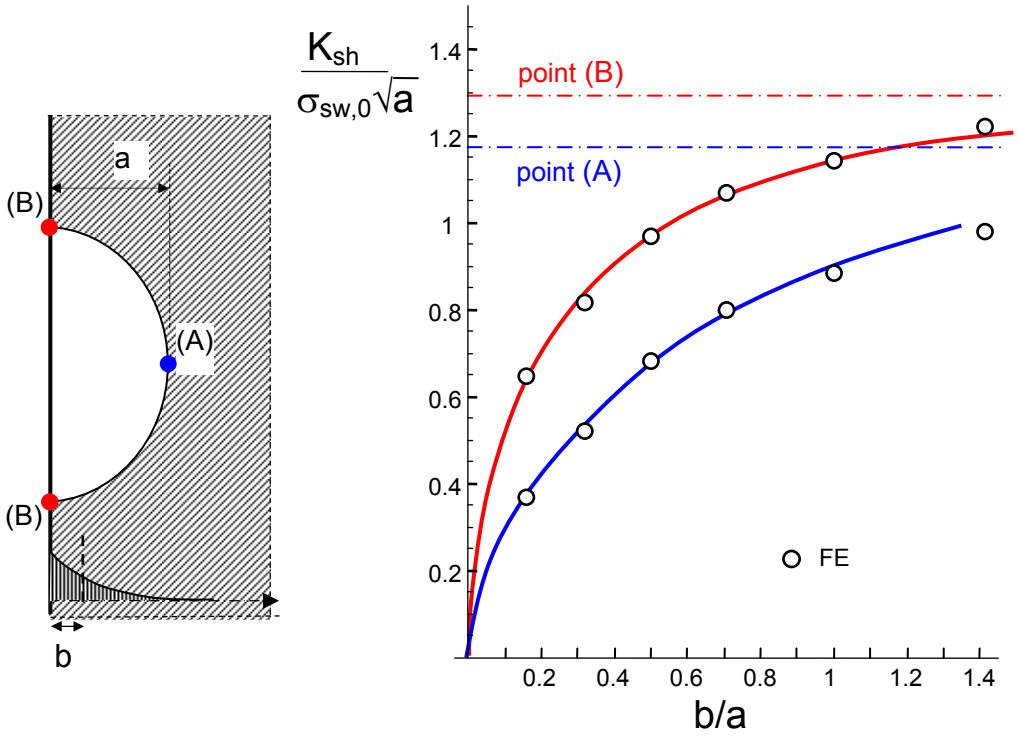

Fig. A3 Shielding stress intensity factors at the deepest point (A) and the surface points (B) of a semi-circular crack in a semi-infinite body.

A3 Semi-circular crack in the half-space via superposition

Two contributions make up the shielding stress intensity factor: one coming from the diffusion zone originating from the crack faces, $K_{sh,1}$, the second originating from the external surfaces of the specimen, $K_{sh,2}$. The total shielding stress intensity factor is the sum of both of these: $K_{sh,A,B} = K_{sh,1} + K_{sh,2}$

<u>*Crack-face zone*</u>: The diffusion zone developing from the crack faces is given by the following equation [12], which holds both at point *A* and point *B*:

$$K_{sh,1} = -\psi \frac{\varepsilon_v E}{1-\nu}\sqrt{b} \tag{A9}$$

The shielding stress intensity factors for points (A) and (B) of the semi-elliptic crack, $K_{sh,2}$, are plotted in Fig. A4 versus a/c and b/a. It is obvious that the shielding stress intensity factor at the surface points (B) is roughly independent of a/c for about $a/c>0.6$. For small b/a, the stress intensity factor $K_{sh,A,2}$ is much less than $K_{sh,B,2}$.

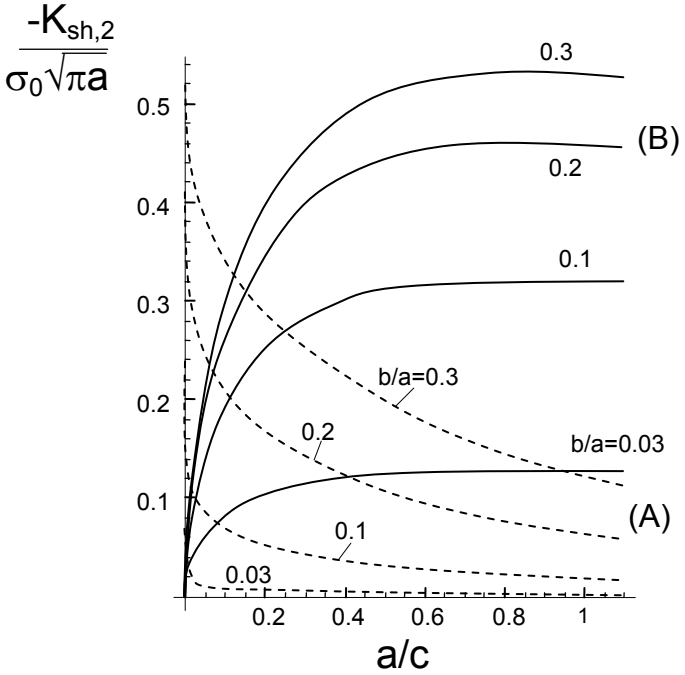

Fig. A4 Influence of aspect ratio a/c and relative depth of the swelling zone b/a on the shielding stress intensity factors $K_{sh,A}$ at the deepest and $K_{sh,B}$ at the surface points of a semi-elliptical surface crack.

This solution can be written as

$$K_{sh,A,B,2} = \sigma_0 \sqrt{\pi\, a}\, F_{A,B} \frac{1.13 - 0.09\sqrt{\frac{a}{c}}\left\{\tanh\left[\left(\frac{a}{c}\right)^{10}\right]\right\}^{1/20}}{\sqrt{1+1.464\left(\frac{a}{c}\right)^{1.65}}} \tag{A10}$$

where $$F_A = \sum_{n=1}^{3} \frac{B_n}{1 + A_1 n \frac{a}{2b} + A_2 \left(n \frac{a}{2b} \right)^2} \tag{A11}$$

and $$F_B = \sum_{n=1}^{3} 1.1 \sqrt{\frac{a}{c}} \frac{B_n}{1 + \left(0.1186 + 0.128 \frac{a}{c} - 0.1134 \frac{a^2}{c^2} + 0.0288 \frac{a^3}{c^3} \right) n \frac{a}{2b}} \tag{A12}$$

The coefficients read

$$A_1 = 0.43 + 0.266 \left(\frac{a}{c} \right)^{0.42} \tag{A13}$$

$$A_2 = 0.266 \left(\frac{a}{c} \right)^{0.42} \tag{A14}$$

$$B_1 = -0.37664, \; B_2 = 2.7314, \; B_3 = -1.35521$$

References:

1. S.M. Wiederhorn, T. Fett, G. Rizzi, S. Fünfschilling, M.J. Hoffmann and J.-P. Guin, "Effect of Water Penetration on the Strength and Toughness of Silica Glass," *J. Am. Ceram. Soc.* **94** (2011) [S1], 196-203.

2. S.M. Wiederhorn, T. Fett, G. Rizzi, M.J. Hoffmann and J.-P. Guin, "The Effect of Water Penetration on Crack Growth in Silica Glass," *Engng. Fract. Mech.* **100** (2013), 3-16.

3. S.M. Wiederhorn, T. Fett, G. Rizzi, M. Hoffmann, J.-P. Guin, "Water Penetration – its Effect on the Strength and Toughness of Silica Glass," *Met. Mater. Trans. A*, **44**(2013) [3], 1164 -1174.

4. T. Fett, G. Rizzi, M. Hoffmann, S. Wagner, and S.M. Wiederhorn, "Effect of Water on the inert Strength of Silica Glass: Role of Water Penetration," *J. Am. Ceram. Soc.* **95**(2012) [12], 3847-3853.

5. H. Li and M. Tomozawa, "Mechanical strength increase of abraded silica glass by high pressure water vapor treatment," *J. Non-Cryst. Solids* **168**(1994), 287-292.

6 A. Zouine, O. Dersch, G. Walter and F. Rauch, "Diffusivity and solubility of water in silica glass in the temperature range 23-200°C," *Phys. Chem. Glass: Eur. J. Glass Sci and Tech. Pt. B*, **48** [2] (2007), 85-91.

7. S. M. Wiederhorn, F. Yi, D. LaVan, T. Fett, M.J. Hoffmann, Volume Expansion caused by Water Penetration into Silica Glass, J. Am. Ceram. Soc. **98** (2015), 78-87.

8 S. M. Wiederhorn, M. J. Hoffmann, T. Fett, Swelling strains from density measurements, Scientific Working Paper **38**, 2015, KIT Scientific Publishing, Karlsruhe.

9. Charles, R.J., Dynamic fatigue of glass, J. Appl. Phys. **29**(1958), 1657–1661.

10 T. Fett, G. Rizzi, M. J. Hoffmann, S. Wagner, S. M. Wiederhorn, Effect of water on the inert strength of silica glass: Role of water penetration, J. Am. Ceram. Soc. **95**(2012), 3847-3853.

11 Fett, T., Failure due to semi-elliptical surface cracks under arbitrary stress distributions. Fatigue and Fracture of Engineering Materials and Structures, **23**(2000) S.347-53

12 McMeeking, R.M., Evans, A.G., Mechanics of Transformation-Toughening in Brittle Materials, J. Am. Ceram. Soc. **65**(1982), 242-246.

13 Fett, T., Munz, D., Stress intensity factors and weight functions, Computational Mechanics Publications, Southampton, 1997.

KIT Scientific Working Papers
ISSN 2194-1629

www.kit.edu